Full Length Article

Experimental investigation on the decomposition of NH_4HSO_4 over V_2O_5-WO_3/TiO_2 catalyst by NH_4NO_3 at low temperature

Ziwen Zheng [a,b], Xuesen Du [a,b,*], Xing Wang [a,b], Yanggu Liu [a,b], Kunlu Chen [a,b], Peng Lu [c,*], Vladislav Rac [d], Vesna Rakic [d]

[a] Key Laboratory of Low-Grade Energy Utilization Technologies and Systems, Ministry of Education of PRC, Chongqing University, Chongqing 400044, China
[b] School of Energy and Power Engineering, Chongqing University, Chongqing 400044, China
[c] Guangdong Province Engineering Laboratory for Air Pollution Control, South China Institute of Environmental Sciences, the Ministry of Ecology and Environment of PRC, Guangzhou 510655, China
[d] Faculty of Agriculture, Department of Chemistry, University of Belgrade, Nemanjina 6, 11080 Zemun, Serbia

ABSTRACT

Deactivation by NH_4HSO_4 deposition is one of the major problems faced by commercial SCR catalysts at low temperatures. In this study, NH_4NO_3 was added to the SCR reaction atmosphere in the presence of H_2O and SO_2 at 250 °C, which is lower than the typical temperatures suitable for the V_2O_5-WO_3/TiO_2 catalyst. After a long test, the catalyst activity decreased from 82 % to 75 %, which is much smaller than the activity drop in the atmosphere without NH_4NO_3. The characterization results indicate that the addition of NH_4NO_3 effectively reduced the deposition of NH_4HSO_4 on the catalyst surface, thus weakening the degree of catalyst poisoning deactivation. In addition, we examined the effect of NH_4NO_3 addition on the regeneration of catalysts deactivated by NH_4HSO_4. The activity of the catalyst deactivated by 5 wt% NH_4HSO_4 recovered efficiently after the deactivated catalyst was treated by NH_4NO_3, NO and O_2 for 1 h at 250 °C. The SEM, FTIR, and BET characterization results reveal the positive effect of NH_4NO_3 in promoting the decomposition of NH_4HSO_4.

1. Introduction

NO_x emission is one of the major causes of atmospheric pollution [1]. SCR (Selective Catalytic Reduction) using NH_3 as a reducing agent is a commonly applied technology for NO_x removal around the world [2]. The standard SCR reaction is as follows:

$$4\ NO + 4\ NH_3 + O_2 \rightarrow 4\ N_2 + 6\ H_2O \tag{1}$$

Currently, most of the commercial SCR catalysts are V_2O_5 loaded on TiO_2 carrier with WO_3 or MoO_3 as additives [3]. These catalysts are often used in flue gases above 320 °C to ensure high NO_x removal activity [4–8]. Once the flue gas temperature decreases, the denitrification activity of the catalyst is significantly inhibited. Moreover, SO_x in the flue gas will react with NH_3 and H_2O to form ammonium sulfate salts such as NH_4HSO_4 (ABS). At low temperature, NH_4HSO_4 is liquid and highly viscous. It adheres to the catalyst surface and continuously traps dust in the flue gas, eventually blocking the catalyst pore and causing severe catalyst deactivation [9–18]. Considering that the flue gas temperature of boilers in non-electric industries is generally lower than the

working temperature of V_2O_5-WO_3/TiO_2 (VWTi) catalyst, it is necessary to develop low-temperature SCR technology. The conventional research to deal with the problems caused by low temperature is through catalyst modification, such as doping Mn [19,20], Ce [21,22] and Cu [23] into the catalyst to solve the lack of low temperature activity. The results of such studies are very promising, but the surface sulfation and NH_4HSO_4 deposition at low temperatures are holding back the application of the low temperature catalysts in filed.

In the 1980 s, kato [24] et al. found that when NO_2 is present and the NO/NO_2 ratio is 1:1, an enhanced SCR reaction occurs as shown in Equation (2), which has a reaction rate more than ten times larger compared to the standard SCR reaction and can maintain higher denitrification efficiency in the low-temperature region (150 °C to 300 °C) and at high GHSV [25].

$$NO + NO_2 + 2\ NH_3 \rightarrow 2\ N_2 + 3\ H_2O \tag{2}$$

This provides a new idea for efficient and stable denitrification in low-temperature sulfur-containing atmosphere. In our preliminary work, it was found that the addition of NO_2 helps to inhibit the

---

generation of NH_4HSO_4 on the catalyst surface and enhance the sulfur resistance of the catalyst, even if the ratio of NO to NO_2 is not 1 [26]. Furthermore, we discovered that NH_4HSO_4 on the surface of the V_2O_5-WO_3/TiO_2 catalyst has high reactivity against NO_x in NO/NO_2 atmosphere. The presence of NO_2 facilitates the decomposition of NH_4HSO_4 on the catalyst surface and recovers the activity of NH_4HSO_4 poisoning catalyst [11,12].

However, more than 95 % of NO_x present in conventional boiler flue gas is in the form of NO, and direct addition of NO_2 to the flue gas is obviously difficult to achieve. It is necessary to screen out suitable additives to induce a change in reaction atmosphere to an enhanced SCR reaction atmosphere. Forzatti [27] et al. effectively improved the low-temperature activity under Fe-ZSM-5 and VWTi catalysts by adding NH_4NO_3 (AN) solution to the conventional atmosphere to induce an enhanced SCR reaction. Bae [28] et al. coupled Sb-doped V-Ti catalysts with NH_4NO_3 solution to achieve efficient and stable denitrification of V-Sb-TiO_2 catalysts under the low-temperature sulfur-containing atmosphere. The reaction is as follows:

$$2 NO + 2 NH_3 + NH_4NO_3 \rightarrow 3 N_2 + 5 H_2O \tag{3}$$
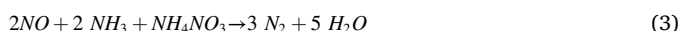
The role of NH_4NO_3 here is to react with NO to produce NO_2 [25,29–32], forming the enhanced reaction atmosphere. Based on previous studies, it is possible to utilize the enhanced SCR reaction for NO_x removal at low temperature. But there are two questions awaiting to be solved, including (1) the adaptability of the NH_4NO_3-enhanced SCR for the commercial V_2O_5-WO_3/TiO_2 catalyst and (2) can the NH_4NO_3-containing atmosphere prevent the deposition of NH_4HSO_4 at low temperatures?

In this work, we added NH_4NO_3 to the SCR atmosphere containing SO_2 and H_2O at low temperature (250 °C) for long time test over the commercial V_2O_5-WO_3/TiO_2 catalyst. Moreover, we investigated the regeneration of the NH_4HSO_4 deactivated catalyst by NH_4NO_3 injection with a combination of a series of characterization techniques. The results indicate that NH_4NO_3 has a positive effect on inhibiting the generation of NH_4HSO_4 on the catalyst surface and accelerating the decomposition of NH_4HSO_4 at low temperatures, thus improving the SO_2 resistance of the V_2O_5-WO_3/TiO_2 catalyst at low temperatures.

2. Experimental

2.1. Preparation of the samples

In this study, V_2O_5-WO_3/TiO_2 catalysts were prepared by the impregnation method. We first dissolved ammonium metavanadate (NH_4VO_3) and ammonium metatungstate ((NH_4)$_6H_2W_{12}O_{40}$) in oxalic acid-acidified water, and then dipped the solution into the TiO_2 carrier with thorough stirring. The mixture was dried at 110 °C for 12 h then calcined in a muffle furnace at 500 °C for 6 h. Finally, the calcined catalyst was ground and sieved to 40–60 mesh for subsequent activity testing and loading with NH_4HSO_4. Mass fractions of V_2O_5 and WO_3 in the V_2O_5-WO_3/TiO_2 catalyst were 1 wt% and 5 wt%, respectively.

NH_4HSO_4 was deposited on the VWTi catalyst using the impregnation method as reported in the literature [33,34]. The amount of NH_4HSO_4 was controlled by varying the concentration in the aqueous solution. After impregnation, the samples were dried at 110 °C for 12 h. The deactivated catalysts were named × wt% ABS-VWTi depending on the amount of NH_4HSO_4 loading. For example, if the mass fraction of NH_4HSO_4 loading was 5 %, the sample was named 5 wt% ABS-VWTi.

2.2. SCR performance measurement

Activity test of the catalyst samples was performed in a quartz tube reactor (Fig. S1). 0.2 g catalyst sample (40–60 mesh) was used for test. The inlet gas mixture contained 500 ppm NO, 500 ppm NH_3, 5 % O_2, 1000 ppm SO_2 (when used), 500 ppm NH_4NO_3 (when used), 2 % H_2O (when used), with N_2 as the balance gas. The total gas flow rate was 1 L/min, corresponding to 300,000 ml/(g*h) of a gas hourly space velocity (GHSV). The temperature was increased from 200 °C to 300 °C with a heating rate of 10 °C/min. The NO_x concentration at the reactor inlet and outlet was measured by a electrochemical analyzer (ecom D, Germany). The catalyst denitrification activity was calculated by the following equation:

$$NO_x \text{ conversion } (\%) = \frac{[NO_x]_{in} - [NO_x]_{out}}{[NO_x]_{in}} \times 100\%$$

$[NO_x]_{in}$ is the NO_x concentration at the reactor inlet and $[NO_x]_{out}$ is the NO_x concentration at the reactor outlet.

2.3. Regeneration of NH_4HSO_4-deactivated catalysts

In this section, the ABS-loaded catalysts were regenerated using different reaction atmospheres at a stable temperature (250 °C). The NO/O_2 atmosphere includes 500 ppm NO, 5 % O_2, and N_2 as balance gas. The $AN/NO/O_2$ atmosphere includes 500 ppm NH_4NO_3, 500 ppm NO, 5 % O_2 and N_2 as balance gas. The total gas flow rate was 1 L/min, which translates into a GHSV of 300000 ml/(g*h). The duration of regeneration treatment was 1 h (4 h and 8 h regeneration results are detailed in the supporting material). The deactivated catalysts after processing in NO/O_2 atmosphere were named × wt% ABS-VWTi @(NO/O_2) and after processing in $AN/NO/O_2$ atmosphere were named × wt% ABS-VWTi @(AN/NO/O_2). The regeneration rate is calculated as follows:

$$\text{Regeneration rate} = \frac{[NO_x \text{ conversion}]_R - [NO_x \text{ conversion}]_p}{[NO_x \text{ conversion}]_F - [NO_x \text{ conversion}]_p}$$

$[NO_x \text{ conversion}]_R$ is the NO_x conversion of the regenerated catalyst. $[NO_x \text{ conversion}]_p$ is the NO_x conversion of the NH_4HSO_4-loaded catalyst. $[NO_x \text{ conversion}]_F$ is the NO_x conversion of the fresh catalyst.

2.4. Catalyst characterizations

FTIR spectra were collected by Nicolet IS10 under ambient pressure. A homogeneous mixture containing the sample and potassium bromide (KBr) was ground and pressed into tablets. Then the IR spectra were collected. The spectra ranged from 4000 to 400 cm^{-1} with a resolution of 4 cm^{-1}. The surface morphology images of the catalyst were taken using a Hitachi SU4800. All SEM images were obtained from secondary electrons with an accelerating voltage of 3 kV. The BET surface area of the catalysts was determined by N_2 adsorption using Mac TriStar II 3020. The samples were degassed at 200 °C for 8 h under vacuum conditions and subsequently measured at 77 K. The crystal structure of the samples was obtained by X-ray diffraction (XRD) from Bruker D8 ADVANCE. The measurement conditions contained: copper K_α radiation; 40 kV/40 mA; scan rate of 5° min^{-1}; and a test range of $2\theta = 10 \sim 90°$. H_2 temperature programmed reduction (H_2-TPR) and NH_3 temperature programmed desorption (NH_3-TPD) results were collected using a PX200A apparatus. For H_2-TPR, 50 mg of samples were pretreated at 120 °C for 1 h under N_2 (50 cm^3/min). After cooling to 100 °C, samples were reduced in H_2/N_2 gas (50 cm^3/min) with temperature increased linearly from 100 °C to 600 °C at the rate of 10 °C/min. For NH_3-TPD, 50 mg samples were pretreated with N_2 (50 cm^3/min) at 120 °C for 1 h. Temperature was lowered to 100 °C for NH_3 adsorption, then purged with N_2 for 1 h after saturation.

3. Results and discussion

3.1. Effect of NH_4NO_3 on SO_2 tolerance of V_2O_5-WO_3/TiO_2 catalyst

Fig. 1 shows the deactivation of the V_2O_5-WO_3/TiO_2 catalyst at 250 °C in the presence of H_2O and SO_2 for long time running. Under the conventional reaction atmosphere (without NH_4NO_3), the NO_x
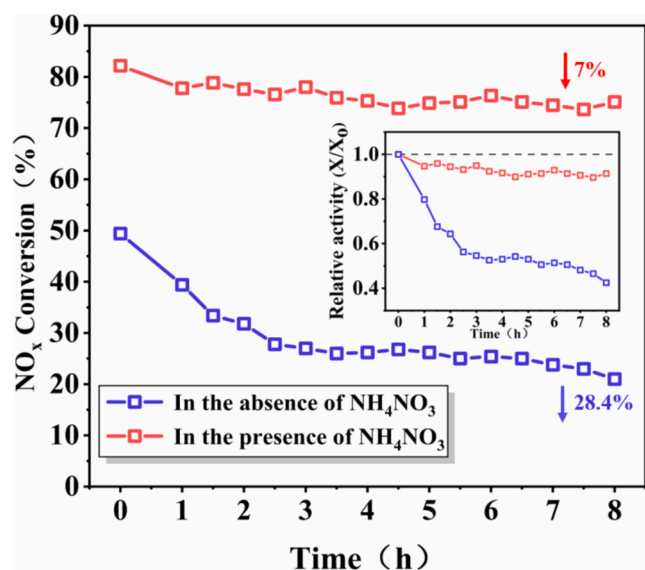
Fig. 1. Effect of NH$_4$NO$_3$ on the VWTi catalyst activity under SO$_2$-containing atmosphere. Reaction conditions: 500 ppm NO, 500 ppm NH$_3$, 1000 ppm SO$_2$, 5 % O$_2$, 2 % H$_2$O, 500 ppm NH$_4$NO$_3$ (when used).

conversion of the catalyst decreased from 49 % to 21 % after 8 h, with a relative decrease of 58 %. In the presence of NH$_4$NO$_3$, the initial catalyst activity dramatically increased from 49 % to 82 % at 250 °C. The NO$_x$ conversion slightly decreased in the first four hours and maintain at a high value after 8 h. Adding NH$_4$NO$_3$ cannot completely prevent the deactivation of the catalyst. But the NO$_x$ conversion in the presence of NH$_4$NO$_3$ only decreased from 82 % to 75 % by 9 % relatively, which is significantly smaller than that in the standard SCR atmosphere. The addition of NH$_4$NO$_3$ at low temperature not only elevates the initial NO$_x$ conversion of the VWTi catalyst, but also enhances the SO$_2$ tolerance of the V$_2$O$_5$-WO$_3$/TiO$_2$ catalyst.

To find out why the NO$_x$ conversion with NH$_4$NO$_3$ injection is supreme to the one without NH$_4$NO$_3$ in the presence of SO$_2$ and H$_2$O, we characterized the processed catalysts by EDS and FTIR. Table 1 shows the atomic ratios of each element for the fresh catalyst and the processed samples (the sample processed under the atmosphere containing NH$_4$NO$_3$ was named VWTi@(AN/SO$_2$/H$_2$O) and the sample processed under the atmosphere without NH$_4$NO$_3$ was named VWTi@(SO$_2$/H$_2$O)). No N and S elements were detected on the surface of the fresh catalyst, while high N content was detected in both VWTi@(AN/SO$_2$/H$_2$O) and VWTi@(SO$_2$/H$_2$O) samples, which may be caused by the adsorption of NH$_3$ on the catalyst surface. The S element content of the VWTi@(AN/SO$_2$/H$_2$O) sample was much smaller than that of the VWTi@(SO$_2$/H$_2$O) sample, which indicates that the addition of NH$_4$NO$_3$ helps to reduce the deposition of NH$_4$HSO$_4$ on the catalyst surface. Less NH$_4$HSO$_4$ deposition on the VWTi@(AN/SO$_2$/H$_2$O) sample than that of the VWTi@(SO$_2$/H$_2$O) sample can be the main reason for the better performance of the NH$_4$NO$_3$ injected atmosphere.

Furthermore, FTIR was used to analyze the surface species of different samples. As shown in Fig. 2, the fresh catalyst shows no visible peaks in the range of 900–1500 cm^{-1}. After processing in the reaction atmosphere containing SO$_2$ and H$_2$O for 8 h, the VWTi@(SO$_2$/H$_2$O) and

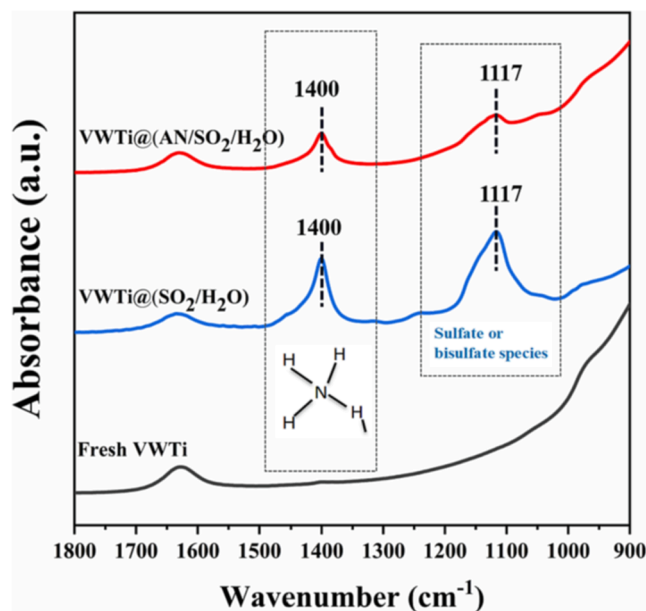**Fig. 2.** FTIR spectra of the fresh VWTi, VWTi@(SO$_2$/H$_2$O) and VWTi@(AN/SO$_2$/H$_2$O) samples.

VWTi@(AN/SO$_2$/H$_2$O) samples show new peaks at 1400 cm^{-1} and 1117 cm^{-1}. The peak at 1400 cm^{-1} can be assigned to the bending vibration of N—H in NH$_4^+$ [11,35,36], and the peak at 1117 cm^{-1} is caused by the stretching vibration of S=O in SO$_4^{2-}$ and HSO$_4^-$ [11,13,34,37]. Both the VWTi@(SO$_2$/H$_2$O), VWTi@(AN/SO$_2$/H$_2$O) samples have high intensity of the bending vibration of N—H at 1400 cm^{-1}, which is generally consistent with the EDS results. Compared with VWTi@(SO$_2$/H$_2$O), VWTi@(AN/SO$_2$/H$_2$O) shows a significant decrease in the vibration intensity of S=O (1117 cm^{-1}). This is because NH$_4$NO$_3$ reacts with NO to form a NO/NO$_2$ mixed atmosphere, which efficiently consumes NH$_3$ in the flue gas and inhibits the formation of ABS [28]. The EDS and FTIR results indicate that the addition of NH$_4$NO$_3$ effectively inhibits NH$_4$HSO$_4$ production on the catalyst surface, thus reducing the extent of catalyst deactivation at low temperature.

3.2. Regeneration of ABS deactivated catalyst

It has been demonstrated above that the addition of NH$_4$NO$_3$ can effectively inhibit the production of NH$_4$HSO$_4$ on the catalyst surface at low temperatures. In this section, NH$_4$HSO$_4$ was pre-loaded on the VWTi catalyst to examine the effect of NH$_4$NO$_3$ on the regeneration of NH$_4$HSO$_4$- deactivated catalyst. Fig. 3 exhibits the standard SCR activity of the fresh, 5 wt% ABS-VWTi, and 10 wt% ABS-VWTi samples. With the increase of NH$_4$HSO$_4$ loading, the catalysts incurred a significant decrease in denitrification activity within the range of 200 °C to 300 °C. Compared to 78 % NO$_x$ conversion of the fresh catalyst at 300 °C, the activity of 5 wt% ABS-VWTi and 10 wt% ABS-VWTi decayed to 45 % and 28 %, respectively.

After regeneration under the NO/O$_2$ atmosphere, the NO$_x$ conversion of 5 wt% ABS-VWTi (Fig. 3 (a)) reached 74 % at 300 °C, which is close to that of the fresh catalyst. The catalyst regeneration rate was 0.88. Nevertheless, the regeneration ability of the NO/O$_2$ atmosphere decreases drastically with the increase of NH$_4$HSO$_4$ loading. As shown in Fig. 3 (b), the NO$_x$ conversion of the 10 wt% ABS-VWTi@(NO/O$_2$) sample was 31 % at 300 °C, which is slightly higher than that of the deactivated catalyst, and the regeneration rate was less than 0.1.

The activity recovery of the ABS-loaded catalyst is more obvious under the AN/NO/O$_2$ atmosphere (Fig. 3). The SCR activity at 280 °C of 5 wt% ABS-VWTi@(AN/NO/O$_2$) has been fully recovered, and the NO$_x$ conversion at 300 °C even exceeds that of the fresh catalyst. This can be

Table 1
Elemental content of catalyst surface after different atmosphere processing by EDS.

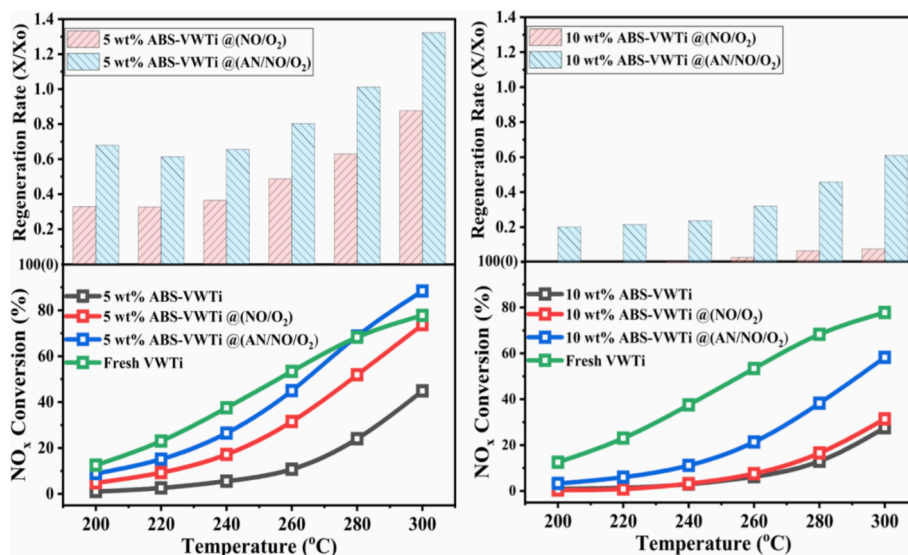| Samples	Ti (%)	V (%)	W (%)	N (%)	S (%)
VWTi	97.5	1.45	1.05	–	–
VWTi@(H$_2$O/SO$_2$)	29.91	0.39	0.47	66.35	2.88
VWTi@(AN/H$_2$O/SO$_2$)	58.95	0.92	0.79	38.83	0.51

Fig. 3. NO_x conversion and regeneration rate after regeneration of the NH$_4$HSO$_4$ deactivated catalysts. (a) 5 wt% NH$_4$HSO$_4$ (b) 10 wt% NH$_4$HSO$_4$.The calculation of the regeneration rate was described in section 2.3. Reaction conditions: 500 ppm NO, 500 ppm NH$_3$, 5 % O$_2$, N$_2$ balance, GHSV = 300000 ml/(g*h).

explained that NH$_4$HSO$_4$ partially decomposes on the catalyst surface after AN/NO/O$_2$ atmosphere treatment, and produces titanium sulfate sites. The generated titanium sulfate can provide acidic sites for NH$_3$ adsorption which promotes the SCR reaction at high temperature [38–41]. The enhanced acidity of the catalyst was also confirmed by NH$_3$-TPD (Fig. 7 (a)). As for the NO_x conversion of 5 wt% ABS-VWTi@ (AN/NO/O$_2$) at low temperature is still lower than that of the fresh catalyst, this is due to the electronic influence caused by strong surface sulfation. The electronic environment of the active sites such as VO_x and WO_x is affected by the adjacent sulfate ions, thus affecting the NO_x conversion at low temperature [11]. In addition, the increase in NH$_4$HSO$_4$ loading weakens the regeneration ability, which is similar to the NO/O$_2$ atmosphere. The NO_x conversion at 300 °C of 10 wt% ABS-VWTi@(AN/NO/O$_2$) recovered to 58 % with a regeneration rate of 0.60 (Fig. 3 (b)).

The effect of processing time on the regeneration effect was also considered. As presented in Fig. S2, the effect of 4 h and 8 h regeneration under the NO/O$_2$ atmosphere is hardly changed. While under the AN/NO/O$_2$ atmosphere, the increase of processing time contributes more to the recovery of catalyst activity. The results of the activity tests suggest that the AN/NO/O$_2$ atmosphere has a greater ability to regenerate ABS-deactivated catalysts than the NO/O$_2$ atmosphere under the same conditions. In the following, characterizations were used to elucidate the regeneration profiles under different atmospheres.

The BET surface areas of the different samples are given in Table 2. Fresh VWTi has the highest BET surface area of 50 m^2/g, which decreases to 40.47 m^2/g after loading 5 % NH$_4$HSO$_4$. Both AN/NO/O$_2$ and NO/O$_2$ atmospheres can make a small recovery of the catalyst specific surface area. The addition of NH$_4$NO$_3$ is more effective for the BET surface area recovery, from 40.47 to 42.07 m^2/g. SEM micrographs clearly show the changes of catalyst surface structure before and after regeneration. As shown in Fig. 4 (a), the porous structure of the fresh catalyst can be easily observed. After loaded with NH$_4$HSO$_4$, the porous

structure of the catalyst gets severely damaged (Fig. 4 (b)). The NH$_4$HSO$_4$ covers the catalyst surface then reduces the surface area. After NO/O$_2$ regeneration, part of the NH$_4$HSO$_4$ decomposes and the pores of the catalyst are re-exposed (Fig. 4 (c)). The AN/NO/O$_2$ regeneration leads a further recovery of the catalyst surface structure (Fig. 4 (d)). However, both reaction atmospheres can hardly recover the specific surface area and surface morphology of the catalyst completely, which explains why the regenerated catalyst activity cannot be fully recovered at low temperatures.

The XRD spectra of the fresh, deactivated and regenerated catalysts are shown in Fig. 5. Anatase is the main crystalline phase of all four samples. 5 wt% ABS-VWTi exhibits no significant change in the crystal structure compared to the fresh catalyst. This is because at low NH$_4$HSO$_4$ loading, ABS is mostly distributed on the catalyst surface in an amorphous form and cannot be detected by XRD means [28]. Even so, the XRD results can still suggest that the crystal structure of the catalyst is not damaged during the impregnation and regeneration of ammonium bisulfate, which ensures the comparability between different samples.

Fig. 6 shows the evolution of surface species before and after the deactivated catalyst was regenerated for 1 h under different atmospheres. Compared to the fresh catalyst (Fig. 2), new peaks appear at 1400 cm^{-1}, 1215 cm^{-1}, 1139 cm^{-1}, and 1044 cm^{-1} for 5 wt% ABS-VWTi. As already mentioned in the previous section, the absorption peak at 1400 cm^{-1} is caused by NH$_4^+$ species. The peaks at 1215 cm^{-1}, 1139 cm^{-1} are attributed to symmetric and asymmetric stretching vibrations of S=O in SO$_4^{2-}$ and HSO$_4^-$ [11,34,42], and the asymmetric stretching vibrations of S—O lead to the peak at 1044 cm^{-1} [11,38,43]. The intensity of the peak near 1400 cm^{-1} of the regenerated sample was significantly weakened until almost disappeared. It indicates that the NH$_4^+$ in NH$_4$HSO$_4$ of the catalyst is mostly consumed by the reaction while the S species partially remain on the catalyst surface as sulfates such as titanium sulfate and vanadium sulfate [11]. Compared to 5 wt% ABS-VWTi, the intensity of the peak at 1045 cm^{-1} slightly decreased for the 5 wt% ABS-VWTi@(NO/O$_2$) sample, and the drop (1041 cm^{-1}) was more obvious for the 5 wt% ABS-VWTi@(AN/NO/O$_2$) sample. This is because the presence of NH$_4^+$ would enhance the asymmetric stretching vibration of S—O—H [11]. After regeneration, the NH$_4^+$ on the catalyst is consumed, which weakened the asymmetric stretching of S—O—H. What's more, NH$_4$NO$_3$ addition weakened the vibrational intensity of S=O through promoting the decomposition of NH$_4$HSO$_4$ [13,28]. As a result, the peak intensity of 5 wt% ABS-VWTi@(AN/NO/O$_2$) sample at 1225 cm^{-1} and 1139 cm^{-1} was much lower than that of 5 wt% ABS-

Table 2
BET surface area of fresh VWTi, 5 wt% ABS-VWTi and regenerated samples with different atmospheres.

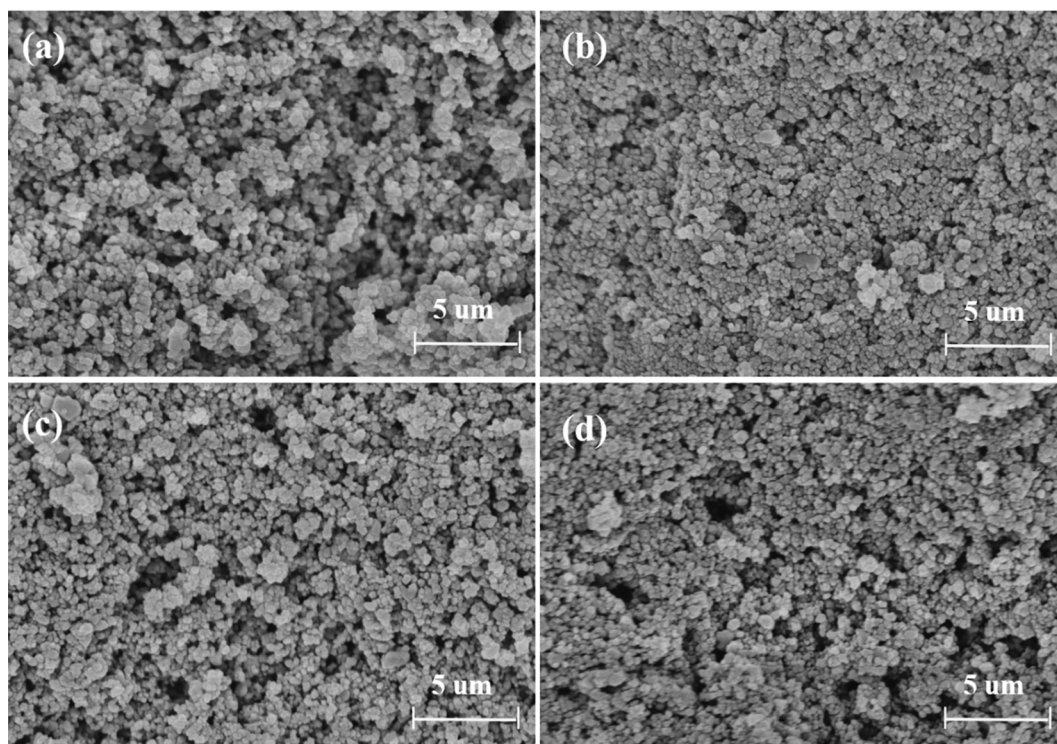| Samples	Fresh VWTi	5 wt% ABS-VWTi	5 wt% ABS-VWTi@(NO/O$_2$)	5 wt% ABS-VWTi@(AN/NO/O$_2$)
BET surface area (m^2/g)	50.00	40.47	41.38	42.07

Fig. 4. SEM microscopic morphology of different samples (a) Fresh VWTi (b) 5 wt% ABS-VWTi (c) 5 wt% ABS-VWTi@(NO/O$_2$) (d) 5 wt% ABS-VWTi@(AN/NO/O$_2$).
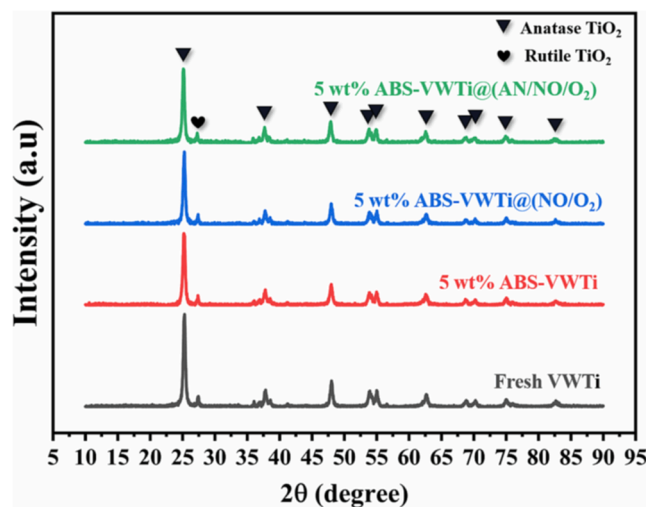

Fig. 5. XRD spectra of the fresh, deactivated and regenerated samples.

Fig. 6. FTIR spectra of 5 wt% ABS-VWTi, 5 wt% ABS-VWTi@(NO/O$_2$) and 5 wt % ABS-VWTi@(AN/NO/O$_2$).

VWTi as well as the 5 wt% ABS-VWTi@(NO/O$_2$) sample.

Fig. 7 shows the NH$_3$-TPD and H$_2$-TPR curves for 5 wt% ABS-VWTi@(AN/NO/O$_2$) and fresh VWTi samples. The NH$_3$-TPD results indicate that the acidity of the regenerated catalyst using AN/NO/O$_2$ atmosphere is obviously stronger than that of the fresh catalyst, which supports that the 5 wt% ABS-VWTi@(AN/NO/O$_2$) sample holds a higher activity at high temperatures. The H$_2$-TPR profile of the fresh catalyst shows a broad reduction peak near 430 °C, which can be attributed to the reduction of V^{5+}. Compared to the fresh catalyst, the reduction peak of 5 wt% ABS-VWTi@(AN/NO/O$_2$) sample shifts toward higher temperatures due to the slight weakening of the redox ability of the catalyst by sulfation.

The above characterization results show that the addition of NH$_4$NO$_3$ accelerates the decomposition of NH$_4$HSO$_4$ on the catalyst surface and further contributes to the recovery of catalyst activity. Therefore, the
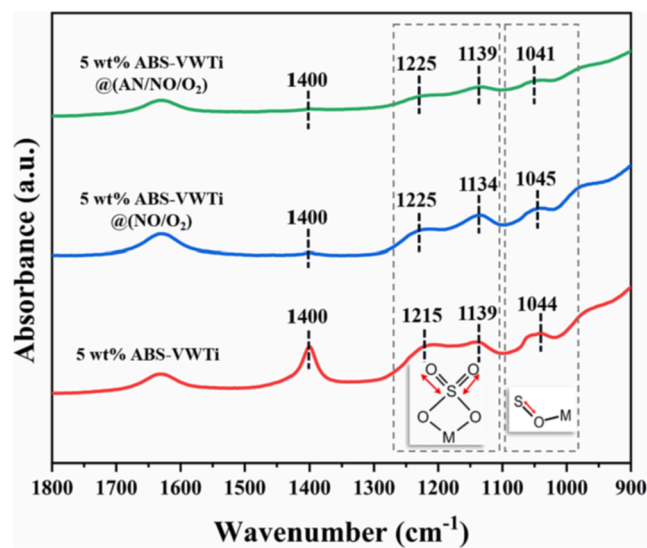
NH$_4$NO$_3$-enhance SCR reaction can effectively uprate the NO$_x$ conversion at low temperatures and also prevent the catalyst surface from covering with NH$_4$HSO$_4$. It is promising to apply the NH$_4$NO$_3$-enhance SCR reaction for NO$_x$ removal at temperatures lower than the appropriate temperatures for standard SCR.

4. Conclusion

Via adding NH$_4$NO$_3$, the denitrification activity and SO$_2$ poisoning resistance of the V$_2$O$_5$-WO$_3$/TiO$_2$ catalyst at low temperatures were enhanced. FTIR and EDS characterizations confirmed that the addition of NH$_4$NO$_3$ attenuated the formation of NH$_4$HSO$_4$ on the catalyst
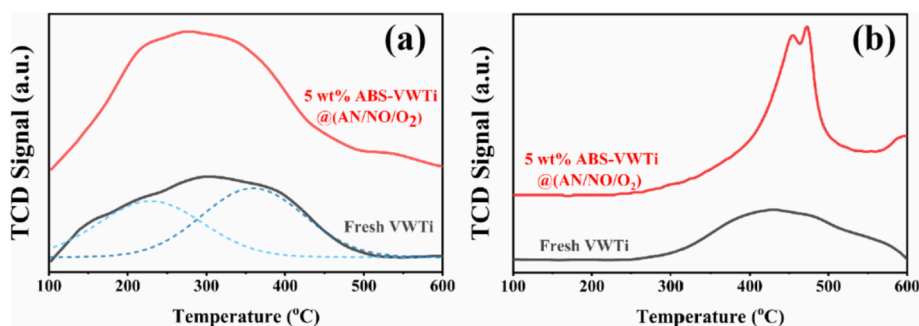
Fig. 7. (a) NH_3-TPD and (b) H_2-TPR profiles for fresh VWTi catalyst and 5 wt% ABS-VWTi@(AN/NO/O_2) samples.

surface. NH_4HSO_4 was loaded directly onto the catalyst, and the NH_4HSO_4-loaded catalyst was regenerated by the NO/O_2 and AN/NO/O_2 atmospheres at 250 °C. The results of activity tests and catalyst characterization reveal that: NH_4NO_3 addition is effective in promoting the decomposition of NH_4HSO_4 on the catalyst surface and restore the activity of the deactivated catalyst. The deactivated catalyst with low NH_4HSO_4 loading is more likely to be regenerated, which means the regeneration process should start early when the catalyst starts to be deactivated in the practical use. In summary, the addition of NH_4NO_3 can not only uprate the NO_x conversion at low temperatures, but also effectively prevent the deposition of NH_4HSO_4 by inhibiting the generation of NH_4HSO_4 and accelerating the decomposition of NH_4HSO_4 on the catalyst surface. Therefore, the NH_4NO_3-enhanced SCR is promising for the NO_x removal in SO_2 and H_2O containing flue gas at temperatures below 300 °C.

CRediT authorship contribution statement

Ziwen Zheng: Investigation, Writing – original draft, Formal analysis. **Xuesen Du:** Validation, Writing – review & editing. **Xing Wang:** Visualization, Resources. **Yanggu Liu:** Supervision, Data curation. **Kunlu Chen:** Project administration. **Peng Lu:** Writing – review & editing, Funding acquisition. **Vladislav Rac:** Writing – review & editing. **Vesna Rakic:** Writing – review & editing.

Declaration of Competing Interest

The authors declare that they have no known competing financial interests or personal relationships that could have appeared to influence the work reported in this paper.

Data availability

Data will be made available on request.

Appendix A. Supplementary data

Supplementary data to this article can be found online at https://doi.org/10.1016/j.fuel.2022.126443.

References

[1] Iwamoto M, Yahiro H, Tanda K, Mizuno N, Mine Y, Kagawa S. Removal of Nitrogen Monoxide through a Novel Catalytic Process. 1. Decomposition on Excessively Copper Ion Exchanged ZSM-5 Zeolites. J Phys Chem 1991;95(9):3727–30.

[2] Iwamoto M, Hamada H. Removal of Nitrogen Monoxide from Exhaust Gases through Novel Catalytic Processes. Catal Today 1991;10(1):57–71.

[3] Choo ST, Yim SD, Nam I-S, Ham S-W, Lee J-B. Effect of promoters including WO3 and BaO on the activity and durability of V2O5/sulfated TiO2 catalyst for NO reduction by NH3. Appl Catal B-Environ 2003;44(3):237–52.

[4] Roduit B, Wokaun A, Baiker A. Global kinetic modeling of reactions occurring during selective catalytic reduction of NO by NH3 over vanadia/titania-based catalysts. Ind Eng Chem Res 1998;37(12):4577–90.

[5] Lai J-K, Wachs IE. A Perspective on the Selective Catalytic Reduction (SCR) of NO with NH3 by Supported V2O5–WO3/TiO2 Catalysts. ACS Catal 2018;8(7):6537–51.

[6] Zhu M, Lai JK, Tumuluri U, Wu Z, Wachs IE. Nature of Active Sites and Surface Intermediates during SCR of NO with NH3 by Supported V2O5–WO3/TiO2 Catalysts. J Am Chem Soc 2017;139(44):15624–7.

[7] Lietti L, Nova I, Ramis G, Dall'Acqua L, Busca G, Giamello E, et al. Characterization and reactivity of V2O5-MoO3/TiO2 De-NOx SCR catalysts. J Catal 1999;187(2):419–35.

[8] Wu R, Li L, Zhang N, He J, Song L, Zhang G, et al. Enhancement of low-temperature NH3-SCR catalytic activity and H2O & SO2 resistance over commercial V2O5-MoO3/TiO2 catalyst by high shear-induced doping of expanded graphite. Catal Today 2021;376:302–10.

[9] Baltin G, Koser H, Wendlandt KP. Sulfuric acid formation over ammonium sulfate loaded V2O5-WO3/TiO2 catalysts by DeNOx reaction with NOx. Catal Today 2002;75(1–4):339–45.

[10] Jangjou Y, Wang D, Kumar A, Li J, Epling WS. SO2 Poisoning of the NH3-SCR Reaction over Cu-SAPO-34: Effect of Ammonium Sulfate versus Other S-Containing Species. ACS Catal 2016;6(10):6612–22.

[11] Wang X, Du X, Zhang L, Chen Y, Yang G, Ran J. Promotion of NH4HSO4 decomposition in NO/NO2 contained atmosphere at low temperature over V2O5-WO3/TiO2 catalyst for NO reduction. Appl Catal A 2018;559:112–21.

[12] Wang X, Du X, Liu S, Yang G, Chen Y, Zhang Li, et al. Understanding the deposition and reaction mechanism of ammonium bisulfate on a vanadia SCR catalyst: A combined DFT and experimental study. Appl Catal B-Environ 2020;260:118168.

[13] Ye D, Qu R, Zheng C, Cen K, Gao X. Mechanistic investigation of enhanced reactivity of NH4HSO4 and NO on Nb- and Sb-doped VW/Ti SCR catalysts. Appl Catal A 2018;549:310–9.

[14] Huang ZG, Zhu ZP, Liu ZY. Combined effect of H2O and SO2 on V2O5/AC catalysts for NO reduction with ammonia at lower temperatures. Appl Catal B-Environ 2002;39(4):361–8.

[15] Muzio L, Bogseth S, Himes R, Chien Y-C, Dunn-Rankin D. Ammonium bisulfate formation and reduced load SCR operation. Fuel 2017;206:180–9.

[16] Chen Y, Li C, Chen J, Tang X. Self-Prevention of Well-Defined-Facet Fe2O3/MoO3 against Deposition of Ammonium Bisulfate in Low-Temperature NH3-SCR. Environ Sci Technol 2018;52(20):11796–802.

[17] Li C, Shen M, Wang J, Wang J, Zhai Y. New insights into the promotional mechanism of ceria for activity and ammonium bisulfate resistance over V/WTi catalyst for selective catalytic reduction of NO with NH3. Appl Catal A 2018;560:153–64.

[18] Xu L, Wang C, Chang H, Wu Q, Zhang T, Li J. New Insight into SO2 Poisoning and Regeneration of CeO2-WO3/TiO2 and V2O5-WO3/TiO2 Catalysts for Low-Temperature NH3-SCR. Environ Sci Technol 2018;52(12):7064–71.

[19] Wang J, Yi X, Ng D, Li H, Miao J, Su Q, et al. Synthesis and Characterization of Mn–Ce–VOx/TiO2 Nanocomposite for SCR of NOx at Low Temperatures: Role of Mn. Ce and V Oxide Top Catal 2020;63(9-10):913–23.

[20] Tang X, Hao J, Yi H, Li J. Low-temperature SCR of NO with NH3 over AC/C supported manganese-based monolithic catalysts. Catal Today 2007;126(3–4):406–11.

[21] Chen M, Zhao M, Tang F, Ruan L, Yang H, Li N. Effect of Ce doping into V2O5-WO3/TiO2 catalysts on the selective catalytic reduction of NOx by NH3. J Rare Earth 2017;35(12):1206–15.

[22] Vuong TH, Radnik J, Rabeah J, Bentrup U, Schneider M, Atia H, et al. Efficient VOx/Ce1−xTixO2 Catalysts for Low-Temperature NH3-SCR: Reaction Mechanism

and Active Sites Assessed by in Situ/Operando Spectroscopy. ACS Catal 2017;7(3): 1693–705.

[23] Shen M, Li C, Wang J, Xu L, Wang W, Wang J. New insight into the promotion effect of Cu doped V_2O_5/WO_3–TiO_2 for low temperature NH_3-SCR performance. RSC Adv 2015;5(44):35155–65.

[24] Kato A, Matsuda S, Kamo T, Nakajima F, Kuroda H, Narita T. Reaction between nitrogen oxide (NO_x) and ammonia on iron oxide-titanium oxide catalyst. J Phys Chem 1981;85(26):4099–102.

[25] Koebel M, Elsener M, Madia G. Reaction pathways in the selective catalytic reduction process with NO and NO_2 at low temperatures. Ind Eng Chem Res 2001; 40(1):52–9.

[26] Wang X, Du X, Zhang L, Yang G, Chen Y, Ran J. Simultaneous Fast Decomposition of NH_4HSO_4 and Efficient NO_x Removal by NO_2 Addition: An Option for NO_x Removal in H_2O/SO_2-Contained Flue Gas at a Low Temperature. Energy Fuel 2018; 32(6):6990–4.

[27] Forzatti P, Nova I, Tronconi E. Enhanced NH_3 selective catalytic reduction for NO_x abatement. Angew Chem Int Ed Engl 2009;48(44):8366–8.

[28] Bae YK, Kim T-W, Kim J-R, Kim Y, Ha K-S, Chae H-J. Enhanced SO_2 tolerance of V_2O_5-Sb_2O_3/TiO_2 catalyst for NO reduction with co-use of ammonia and liquid ammonium nitrate. J Ind Eng Chem 2021;96:277–83.

[29] Nova I, Ciardelli C, Tronconi E, Chatterjee D, Bandl-Konrad B. NH_3–NO/NO_2 chemistry over V-based catalysts and its role in the mechanism of the Fast SCR reaction. Catal Today 2006;114(1):3–12.

[30] Ciardelli C, Nova I, Tronconi E, Chatterjee D, Bandl-Konrad B. A "Nitrate Route" for the low temperature "Fast SCR'' reaction over a V2O5-WO3/TiO2 commercial catalyst. Chem Commun 2004;23:2718–9.

[31] Ciardelli C, Nova I, Tronconi E, Chatterjee D, Bandl-Konrad B, Weibel M, et al. Reactivity of NO/NO_2-NH_3 SCR system for diesel exhaust aftertreatment: Identification of the reaction network as a function of temperature and NO_2 feed content. Appl Catal B-Environ 2007;70(1-4):80–90.

[32] Yeom Y, Henao J, Li M, Sachtler W, Weitz E. The role of NO in the mechanism of reduction with ammonia over a BaNa-Y catalyst. J Catal 2005;231(1):181–93.

[33] Zhu ZP, Niu HX, Liu ZY, Liu SJ. Decomposition and reactivity of NH_4HSO_4 on V_2O_5/AC catalysts used for NO reduction with ammonia. J Catal 2000;195(2): 268–78.

[34] Ye D, Qu R, Song H, Gao X, Luo Z, Ni M, et al. New insights into the various decomposition and reactivity behaviors of NH_4HSO_4 with NO on V_2O_5/TiO_2 catalyst surfaces. Chem Eng J 2016;283:846–54.

[35] Shi Y-J, Shu H, Zhang Y-H, Fan H-M, Zhang Y-P, Yang L-J. Formation and decomposition of NH_4HSO_4 during selective catalytic reduction of NO with NH_3 over V_2O_5-WO_3/TiO_2 catalysts. Fuel Process Technol 2016;150:141–7.

[36] Zhang L, Li L, Cao Y, Yao X, Ge C, Gao F, et al. Getting insight into the influence of SO_2 on TiO_2/CeO_2 for the selective catalytic reduction of NO by NH_3. Appl Catal B-Environ 2015;165:589–98.

[37] Ye D, Qu R, Song H, Zheng C, Gao X, Luo Z, et al. Investigation of the promotion effect of WO3 on the decomposition and reactivity of NH_4HSO_4 with NO on V_2O_5–WO_3/TiO_2 SCR catalysts. RSC Adv 2016;6(60):55584–92.

[38] Ropero-Vega JL, Aldana-Perez A, Gomez R, Nino-Gomez ME. Sulfated titania $[TiO_2/SO_4^{2-}]$: A very active solid acid catalyst for the esterification of free fatty acids with ethanol. Appl Catal A 2010;379(1–2):24–9.

[39] Arfaoui J, Boudali LK, Ghorbel A, Delahay G. Effect of vanadium on the behaviour of unsulfated and sulfated Ti-pillared clay catalysts in the SCR of NO by NH_3. Catal Today 2009;142(3–4):234–8.

[40] Khalfallah Boudali L, Ghorbel A, Grange P. Characterization and reactivity of WO_3–V_2O_5 supported on sulfated titanium pillared clay catalysts for the SCR-NO reaction. C R Chim 2009;12(6–7):779–86.

[41] Xiao X, Xiong S, Shi Y, Shan W, Yang S. Effect of H_2O and SO_2 on the Selective Catalytic Reduction of NO with NH_3 Over Ce/TiO_2 Catalyst: Mechanism and Kinetic Study. J Phys Chem C 2016;120(2):1066–76.

[42] Mamlouk M, Ocon P, Scott K. Preparation and characterization of polybenzimidzaole/diethylamine hydrogen sulphate for medium temperature proton exchange membrane fuel cells. J Power Sources 2014;245:915–26.

[43] Noda LK, de Almeida RM, Probst LFD, Gonçalves NS. Characterization of sulfated TiO_2 prepared by the sol–gel method and its catalytic activity in the n-hexane isomerization reaction. J Mol Catal A-Chem 2005;225(1):39–46.